SERS-Active Photonic Crystal Fiber Probe: Towards Next Generation Liquid Biopsy Sensor with Ultra High Sensitivity

Dinish U. S[1,*], *Flavien Beffara*[1,2], *Georges Humbert*[2,*], *Jean-Louis Auguste*[2], *Malini Olivo*[1,*]

[1] Lab of Bio-Optical Imaging, Singapore Bioimaging Consortium (SBIC), Agency for Science Technology and Research (A*STAR), Singapore

[2] XLIM Research Institute, UMR 7252 CNRS / Limoges University, 123 av. A. Thomas, 87060, Limoges, France

* Corresponding Authors:

dinish@sbic.a-star.edu.sg; georges.humbert@xlim.fr; Malini_Olivo@sbic.a-star.edu.sg

Abstract

The tremendous enhancement factors that Surface Enhanced Raman Scattering (SERS) possess coupled with the flexibility of photonic crystal fibers (PCFs) paves the way to a new generation of ultrasensitive biosensors. Thanks to the unique structures of PCFs, which allows direct incorporation of analyte into the axially aligned air channels, interaction between the analyte and excitation light could be increased many folds leading to flexible, reliable and sensitive probes that can be used in preclinical or clinical biosensing. SERS-active PCF probes provides unique opportunity to develop an opto-fluidic liquid biopsy needle sensor that enables one-step integrated sample collection and testing for disease diagnosis. Specificity being a key parameter to biosensors, the PCF inside the biopsy needle could be functionalized with targeting moieties to detect specific biomarkers. In this review paper, we present some of the most promising recent biosensors based on PCFs including hollow-core PCFs, suspended-core PCFs and side-channel PCFs. We provide a wide range of applications of such platform using Raman spectroscopy, label free SERS or labelled SERS detection and analyze some of the main challenges to be addressed for translating it to a clinically viable next generation sensitive biopsy needle sensing probe.

1. Introduction

Raman spectroscopy, which relies on inelastic scattering of light, is a rapid, non-destructive optical technique that probes vibrational modes of a molecule. It allows clear determination of molecules and molecular structures as each one has its own distinct vibrational modes, or "fingerprints". Moreover, the narrow spectral bands allow to distinguish various bio-chemical species making Raman spectroscopy highly selective [1]–[4]. However, this technique lacks the

This article has been accepted for publication and undergone full peer review but has not been through the copyediting, typesetting, pagination and proofreading process, which may lead to differences between this version and the Version of Record. Please cite this article as doi: 10.1002/jbio.201900027

sensitivity due to i) extremely low efficiency of Raman scattering process and ii) the photons are scattered in all directions, thus largely limiting the intensity of the signal detected by a spectrometer [5].

Over the past two decades, Surface Enhanced Raman Scattering (SERS) has become more popular for various preclinical and clinical biosensing applications [6]–[15]. In SERS, when analyte molecules are adsorbed onto nano-roughened plasmonic metal surfaces of silver/gold (Ag/Au) or their colloidal nanoparticles (NPs), scattered signals can be enhanced by several orders of magnitude (~10^8-10^{14}), thus overcoming the sensitivity limitation of Raman scattering [16]–[20]. This greatly facilitate the molecular detection while preserving their unique "fingerprint". Usually, nano-roughened substrates are fabricated on planar platforms such as glass or silicon, but this limits the interaction area between excitation laser and sample to almost two dimensions. Effective SERS enhancement appears mainly in the first 100 nm away from the nanostructures and limits the interaction area, therefore compromising the ability to detect trace amount of biochemical species [21]–[24].

To address this limitation, recently, photonic crystal fibers (PCFs) with axially aligned air channels running along the entire length of the fiber are being explored to provide an excellent platform for SERS biosensing [4], [25]–[27]. They enable the incorporation of metallic NPs and liquid-analytes into their air holes and thereby increases the interaction area between the guided light and the analyte [28]–[30]. Moreover, PCFs exhibit relatively low-loss transmission making them ideal to guide both excitation and Stokes shifted Raman signals. In this way, the fiber can simultaneously function as an excitation and collection platform. Also, since the sample is contained within the sensing medium, real-time monitoring is possible, making PCF-based sensor particularly attractive for biosensing in both preclinical and clinical settings. Such a configuration enables biosensing at extremely low sample volume (nL) and provides very high sensitivity of the order of pM for the detection of biomarkers [2], [4], [25], [31]. SERS-active PCF probes offer at least 2-3 orders higher sensitivity than conventional sensing on planar substrates, which is highly significant in the context of biosensing [3], [27], [32].

This review aims to provide an overview and critical analysis of the recent developments in various SERS-active PCF designs for biosensing. This involves the innovative designs of hollow-core PCFs and solid-core PCFs. Theoretical analyses in the fiber designs to achieve highly sensitive biosensing using SERS will also be discussed. We give a detailed account of some of the most promising applications of SERS and Raman-active PCF probe for label free and labelled detection of biomarkers and bio-analytes with very high sensitivity. This review will be concluded by commenting on the challenges to be addressed in developing a reliable SERS-active PCF liquid biopsy needle sensor for future clinical applications that act as an opto-fluidic platform with integrated sample collection and testing. Such a sensor could find tremendous application in sensitive biomarker sensing as compared to conventional biopsy needle, which requires two step sensing approach.

2. Fiber designs used in SERS based biosensing

The recent advancement in PCF technology has enabled the development of novel opto-fluidic platforms. The tiny air holes of PCFs could serve as natural liquid-chambers enabling improved light-analyte interactions over extremely large length, leading to unparalleled signal enhancement and hence detection sensitivity. The flexibility of the fabrication process resulted in the development of numerous novel PCF designs composed of a hollow core or a solid core [33]–[35]. In the following sections, we introduce the main properties, interests and drawbacks of the different PCFs that are used for Raman and SERS based sensing applications.

2.1 Hollow-core fiber

In hollow-core fibers, sensing is realized by filling at least the central core with the liquid-analyte and then by guiding the light within this hollow core. This configuration offers complete light-analyte interaction over the core and along the length that is limited by the absorption coefficient of the analyte and the attenuation coefficient of the fiber. Hollow-core fibers offer SERS sensing without parasitic Raman signals from the fiber material, since light is propagated in the inner hollow core where analyte is residing.

One class of such fiber is composed of a hollow core surrounded by a photonic crystal cladding of 2-dimensional pattern of air holes with an extremely large air filling fraction (> 94%), as shown in Figure 1(a) [36]. Within a specific wavelength range, the cladding exhibits photonic bandgap (PBG) properties, i.e. light propagation is forbidden in the cladding, enabling light confinement in the hollow core alone within a specific transmission window that depends on the cladding topology. This fiber, which is called HC-PCF, exhibits a rather low attenuation coefficient (with a record of 1.2 dB/km) making it an excellent platform for enhancing light interactions with gases or liquids over a large length and within a confined area (with core diameter typically of about 10 µm to 20 µm for a transmission windows around the wavelength of 1.5 µm) [37]. However, HC-PCFs suffer from several drawbacks that limit their use for SERS based biosensing and other opto-fluidic applications such as: (i) transmission window is rather narrow ($\Delta\lambda/\lambda \sim 0.08$ with $\Delta\lambda$ is the transmission window and λ the center wavelength) and it is spectrally shifted with the refractive index of the liquid infiltrated into the HC-PCF [38], [39], (ii) the proprieties (ex. transmission window) could be deteriorated by light coupling to modes confined in the ring of glass surrounding the hollow core [40] and (iii) SERS based biosensing performance is reduced by the drop in the light intensity near the inner surface of the hollow core, where metallic NPs and SERS-active NPs (SERS nanotags) have to be anchored for labelled real-life sensing applications.

Another class of hollow-core fiber is composed of a photonic crystal with a Kagome lattice (Figure 1 (b)). In contrast to earlier mentioned HC-PCF, in this fiber, light is confined in the hollow core by the anti-resonant guiding mechanism with inhibited coupling to cladding modes [41]. In comparison with HC-PCF, this guiding mechanism yields broader transmission window, making them less sensitive to the refractive index of the liquid infiltrated into the channels. However, this fiber known as “Kagome HC-PCF” exhibits larger attenuation coefficient, larger bend losses and stronger decay of the field before the inner core surface (~30 dB) than HC-PCF (~20 dB) [41]. It is worth noting that SERS based biosensing has only been demonstrated using fibers composed of PMMA material [28], even if silica based Kagome HC-PCF exhibits better properties that have been exploited for in-fiber liquid spectroscopy and generation in stimulated Raman scattering [41]–[43].

HC-PCFs could also be used for propagating light only in a liquid core, by total internal reflections (TIR), when the refractive index of the liquid (infiltrated into the hollow core) is higher than the effective index of the cladding (filled with air), as shown in Figure 1(c) [44]. This configuration is called "liquid-core HC-PCF", which enables a very large transmission window and higher light interaction with analyte in the inner surface of the core. However, light guidance is generally highly multimode in contrast to the conventional HC-PCFs where both core and cladding are filled and it requires specific techniques for selectively filling only the central hollow core with a liquid, making liquid-core HC-PCFs hardly compatible with real-life sensing applications.

It is worth noting that liquid-core fiber could also be realized without photonic crystal cladding. R. Altkorn *et al.* have fabricated a liquid-core fiber, which is simply composed of polymer capillaries of Teflon-AF 2400 that has a lower refractive index (n = 1.29) than the water for enabling TIR guidance [45]. Nevertheless, the thermo-mechanical properties of this material limits the fabrication of uniform and small core (~ 0.5 mm diameter) fiber samples leading to large attenuation of light (~4 dB/m for a water core) and highly multimode guiding regime. Furthermore, the development of this fiber is limited by the cost of the material (10 000 $ / Kg).

2.2 Solid-core fiber

SERS sensing with a solid-core PCF (SC-PCF) is realized through the interactions between the evanescent part of the guided light and the analyte (including NPs and Raman reporters). The amount of the evanescent light is generally increased significantly by reducing the core diameter of the fiber down to the size of the wavelength or even below. In this prospect, fiber tapers fabricated by heating and stretching of small part of a standard optical fiber are ideal components since a very small core (down to sub-micrometer) could be obtained and they enable efficient light injection and collection through the un-tapered part of the fiber (both ends of the taper) [46]. However, they suffer from their brittleness, sensitivity to dusts, limited length (tens of centimeters), and they are not compatible with in-fiber opto-fluidic system. These constraints are solved with SC-PCFs that could even be coiled for making compact devices. Consequently, the SC-PCFs developed for in-fiber opto-fluidic sensing tend to reproduce the fiber taper configuration by associating air/liquid channels in the vicinity of a small core, but at the expense of a degraded light coupling efficiency

when the core diameter becomes very small. In the following section, we highlight different families of SC-PCF used for SERS based biosensing applications.

Standard SC-PCFs are composed of silica core surrounded by a periodic array of air holes (photonic crystal) embedded in a silica cladding [47], as shown in Figure 2 (a). It is worth noting that silica could be replaced by another glass. By carefully controlling the ratio of the diameter of the holes and the pitch (Λ) of the photonic crystal cladding, light guided in the core could exhibit remarkable properties such as extremely large evanescent field, endlessly single mode propagation and tailored group velocity dispersion curve. However, light-liquid interactions require small core leading to fibers with small hole diameter, which in turn strongly limit the practical liquid infiltration.

Suspended-core PCFs (SuC-PCFs) are composed of a small silica core surrounded by few large air channels for enabling efficient liquid infiltration (Figure 2 (b), 2(c)). The shape of the core is triangular, square or circular depending on the number of capillaries, 3, 4, or 6 respectively, with round shape in the vicinity of the struts. The properties of the fiber tend to be of a silica rod in the air. The fraction of evanescent light in the air hole is increased by simply reducing the core size. However, light is guided in multimode regime with light-field extending in the silica struts [48], excepted for small core diameter (below 1 µm). Therefore, this multimode regime requires meticulous experimental conditions to launch light in the same mode for realizing reliable and stable SERS based measurements.

Side-channel PCF (SiC-PCF) is a new class of PCF that associates the advantages of SC-PCF and SuC-PCF as shown in Figure 2 (d), 2(e) and 2(f). Such fiber is composed of a silica core partially surrounded by a photonic crystal. A portion of the photonic crystal is removed to form a large air channel on the side of the core. The photonic crystal and the air channel enable a tight control of the properties of the guided light such as single mode propagation, and an efficient liquid infiltration [49]. SiC-PCF is therefore very suitable for in-line opto-fluidic lab-in-fiber applications [50]. It is nevertheless more complicated to fabricate than conventional SC-PCF or SuC-PCFs.

Core-array PCF is an alternative option that is composed of an array of small cores (hold by silica struts) yielding a high fraction of evanescent light and larger surface-area of interactions

between the light and the analyte. Such fiber could be realized by exploiting the small cores formed at the interstices of the holes in the photonic crystal of a PCF (Figure 2 (g)) [47], [51], by fabricating a PCF without a core [52], or by drawing down a commercial multi-hole capillary preform to a fiber (Figure 2(h), 2(i) [53]). However, light is propagated in highly multimode regime, leading to less controlled and repeatable measurements, higher propagation losses (~ 1 dB/cm [52], [53]), and higher loss of light at the input and collection (~ 28 dB [52]) side in these fibers.

3. Applications of Raman/SERS-active PCF probes

SERS-PCF probes have been used to successfully detect and quantify several important biological analytes. In the following sections, we review some of the most promising applications of SERS/Raman-active PCF biosensors. Initially, to study the performance of various fiber designs and efficacy of NP anchoring into the fiber, several studies were conducted using common Raman active molecules as model analyte. Then, we review some of the most promising bio-chemical sensing based on label free Raman, label free SERS and labelled SERS approach. Finally, to further emphasize the enormous possibilities of Raman-active PCF probes, we review two promising gas sensors based on this technology. A summary of all these applications is provided in table 1.

3.1 Evaluating the performance of SERS-active PCF probe using a common Raman reporter molecule

Rhodamine 6G (Rh6G) is a highly fluorescent dye that is commonly used as a Raman reporter molecule. It was first used to evaluate the effectiveness of an HC-PCF (modified into a liquid-core HC-PCF by sealing the cladding holes before filling liquid in to the core by capillary action) as a SERS platform when mixed with AgNPs, resulting in an improved signal enhancement by a factor of 100 compared to a sample dried on a planar substrate using a 785 nm laser [54]. Tiwari *et al.* compared the Raman signal from different lengths of HC-PCF (HC-1550 Thorlabs) that had been non-selectively filled with analyte [32]. Rh6G solution was mixed with AgNPs in a 1:1 volume ratio before filling HC-PCFs with 6 different lengths by capillary action. A reservoir of the mixture was attached at the end of the fiber to ensure that analyte did not dry out and a 785 nm laser was

used as excitation source. The lengths of the fiber used in this study varied from 4.7 to 8 cm, increasing in 5 mm steps. The intensity of the 1357 cm^{-1} peak of Rh6G was compared for each fiber and it was found that the signal enhancement was directly proportional to the fiber length, increasing from 4.7 to 6.5 cm and then saturating at longer lengths. As the length of the fiber directly correlates to the amount of sample that it could be contained within, this also indicates that the signal enhancement increases linearly with increasing the sample volume due to more light-sample interaction. A separate experiment was also carried out to determine the individual contributions of the HC-PCF and the NPs towards signal enhancement, with an enhancement of ~16 times from the HC-PCF alone while ~20 times enhancement due to the NPs alone, leading to a global enhancement of approximately 300 times.

Later, Oo *et al.* used Rh6G as a model analyte to experimentally compare three different types of PCFs for their potential application in evanescent-field based Raman spectroscopy after modelling them using numerical simulation and hyperspectral Raman imaging [55]. The three fibers used in this study were SC-PCF with a core of 2.6 µm and surrounded by 6 rings of air channels and two SuC-PCFs with a core diameter of 3.1 µm and 1.1 µm surrounded by three air channels. The excitation laser operated at 632.8 nm. A 24 cm long PCF was cut and AgNPs (diameter ~35 nm) were immobilized onto the inner walls of the cladding air channels, with a density of ~0.2 NPs/μm^2. It was found that SuC-PCF with the smallest core size was the most sensitive, providing a detection sensitivity of $1x10^{-10}$ M.

Zhang *et al.* recently could achieve a record low concentration of 50 fM of Rh6G when mixed with AuNPs in a 1:1 ratio using a specially designed SiC-PCF and excited at 632.8 nm [49]. They also studied the impact of the fiber length on the Raman intensity. They showed that for backscattering setup, an optimal fiber length exists after which the signal increment with the fiber length is negligible, as shown in Figure 3. In addition, the role of the concentration of AuNPs as a function of fiber length was also investigated and demonstrated that at higher NP concentration SERS intensity reaches a plateau at shorter length.

As mentioned previously, Guo *et al.* designed a flow-through multi-holes capillary which can be seen as an array of small cores separated by 2.9 µm holes (Figure 2 (h), 2(i)) [53]. This design

allows a larger fraction of evanescent field and surface area for interaction. Without optimizing the excitation laser wavelength (785 nm), the length of fiber and the coverage density of NP, they managed to detect concentrations lower than 100 fM and achieved an enhancement factor of 10^8. After optimization, this device may potentially lead to one of the most powerful biosensing platforms. However, one should keep in mind that such configuration suffers from high coupling losses and may lead to relatively poor repeatability in measurements as the light is guided in highly multimode regime.

3.2 Sensing of biologically relevant molecules

3.2.1 Label free Raman detection

In this section, analyte that inherently possess high Raman scattering cross section and incorporated directly into the PCF are discussed. These analytes were detected using classical Raman spectroscopy without the signal enhancement using NPs.

Heparin

Heparin is a blood anticoagulant, which is administered before and during cardiac surgery or dialysis and can lead to serious bleeding if its dosage is not controlled. As such, it is very important for surgeons to accurately and rapidly monitor heparin levels in blood. Current methods include activated clotting time (ACT), Anti-Xa assay and activated partial thromboplastin time. Out of these, ACT is considered as the gold standard for sensing heparin. It measures the time taken for a fibrin clot to form after exposing whole blood to specific clotting agents and it can take up to 180 seconds, which is not ideal in a surgical environment. In addition, delays in performing heparin measurements can also lead to inaccurate results [26], [56], [57]. Lab-based techniques for quantifying heparin include fluorescence, surface plasmon resonance (SPR) and membrane-based ion-selective electrodes, which are complicated and may lead to inaccurate results as they depend on identifying cross-reaction products of heparin with labelling agents.

Khetani *et al.* demonstrated the detection of heparin level in blood using a five centimeter long HC-PCF (HC-1550-04, NKT Photonics) [56]. The PCF holes were manually and non-selectively filled with varying concentrations of serum-heparin mixture using a syringe and air gaps in the sample caused by evaporation due to laser irradiation (785 nm) was controlled by continuously replenishing the sample from an in-house reservoir. Schematic of the typical signal collection in backscattering mode generally used with PCF sensors is shown in Figure 4. Khetani *et al.* showed that the intensity of the 1005 cm^{-1} Raman peak of heparin varied linearly with its concentration, as shown in Figure 5. In addition, the HC-PCF was found to exhibit strong modal-field overlap with the heparin-serum mixture, resulting in a Raman signal enhancement of 90 times with a detection limits of 12 USP/mL (USP refers to United States Pharmacopeia and describes the potency of a drug in clinical applications), which is within the clinically relevant level. Additionally, the sample required was within microliter level, which indicates the tremendous potential as a clinical sensing tool for rapid and accurate determination of heparin levels in small volume of sample. In this study, it is worth noting that no direct detection of heparin from whole blood has been conducted.

Glucose

The accurate measurement and monitoring of blood glucose levels is of paramount importance to prevent hypo- or hyperglycemia for those with diabetes mellitus. The most common form of glucose monitoring technology is the “finger-prick” type of device, which is inconvenient and it indirectly measures blood glucose through electrochemical means. In one of the earlier attempts to realize a PCF probe for glucose using, Yang *et al.* filled an eight cm long HC-PCF (Air-6-800, NKT Photonics) with aqueous glucose solution within the physiologically relevant concentrations by capillary action [2]. They measured the Raman signal of glucose solution (~50 nL) with a laser power of 2 mW at 632.8 nm excitation and with an integration time of 30 s. This Raman active-PCF sensor could detect glucose within the range of 0-25 mM and its measurement time was much shorter and could achieve superior sensitivity than that was previously reported using high power laser excitation [58], [59]. Additionally, Raman spectroscopy was able to clearly distinguish glucose from fructose, showing the high molecular specificity, as shown in Figure 6. Generally, glucose possess very weak Raman cross section and reported sensitivity in this study is worth noting. This study is particularly promising for future research into developing a sensitive glucose

sensor. However, more optimization and detailed studies are required to achieve a better dynamic range in measurement to yield a clinically viable glucose sensor.

Antibiotics (moxifloxacin)

Monitoring of antibiotics levels in body fluids can be of tremendous importance for patients with severe sepsis and septic shocks as a rapid dose adjustment is primordial for their survival. In this context, Yan *et al.* successfully detected moxifloxacin using a HC-PCF (NKT Photonics) probe [31]. The light was guided in TIR regime by filling only the core of the fiber with the aqueous solution (liquid-core HC-PCF) leading to a wide transmission window from UV to near infrared. In this configuration, they were able to enhance the Raman signal of moxifloxacin using several excitation wavelengths such as 532 nm, 676 nm and 752 nm demonstrating the benefit of a wide transmission window. Moxifloxacin possesses two intense Raman peaks at 1373 cm^{-1} and 1620 cm^{-1} that are suitable for low concentration detection. They recorded the intensity variations of the 1620 cm^{-1} peak with the concentrations of moxifloxacin in order to predict the concentration of an unknown solution. Finally, they succeeded in detecting moxifloxacin up to 1.7 µM in a 4 nL sample, making this device very promising for biosensing as it required only a very small volume of analyte and the measured concentration was within medically relevant range.

3.2.2 Label free SERS detection

In this section, sensing of bio-analytes using AgNPs or AuNPs, which are anchored inside the inner walls of PCF in a controlled manner to realize SERS based detection of analytes, are discussed. Bio-analytes such as adenosine and leukemia cells were studied using this approach.

Adenosine

Adenosine is an important molecule from a clinical standpoint, as it regulates extracellular physiological activity. For patients with asthma and choric obstructive pulmonary disease (COPD), it affects tissue destruction during bronchoconstriction. Current methods for detecting adenosine,

such as high-performance liquid chromatography with UV/fluorescence or enzyme-based amperometry are not ideal. They may cause tissue damage and moreover the approach is complex and indirect. Khetani *et al.* first acquired the SERS spectrum of adenosine using AgNPs in a quartz cuvette using a 785 nm laser excitation. Then, they non-selectively filled a six cm long HC-PCF (HC-1550-04, NKT Photonics) with the same mixture and they showed that the intensity of the ~733 cm^{-1} peak of adenosine was 90 times stronger than that measured with the cuvette [60]. Finally, they could establish that an overall enhancement of ~2700 was achieved with this sensor as compared to cuvette measurement, showing the utility of SERS-active PCF probes in biodetection.

Leukemia cells

Acute myeloid leukaemia (AML) is blood cancer in bone marrow, where normal blood production is affected and abnormal immature white blood cells takes its place. AML progresses rapidly and can lead to anaemia, bleeding problems, infection and it is one of the leading cause of disease-based morbidity in children and adolescents. The early detection of AML and the determination of minimal residual disease is thus very important; however, current techniques such as flow cytrometry and immunohistochemistry are both time-consuming and expensive. To address this problem, a proof of concept study was conducted using a HC-PCF (HC19-1550, NKT Photonics) with a 20 µm core and it was filled with a mixture of cultured HL60 cells and 60 nm AgNPs [27]. The NPs were found to enhance the Raman signal by a factor of approximately 2700 (Figure 7 (a)) at 785 nm excitation. The Raman spectra of cells at different stages (necrotic, apoptotic, and live) were measured and exhibited clear differences. When combined with statistical analysis, this method could successfully differentiate between these three stages. Finally, a calibration curve was obtained (Figure 7 (b),(c)) by measuring six samples at different concentrations of leukemia cells repeated over ten times. This yielded a detection sensitivity as low as ~300 cells/mL, making this HC-PCF probe as a highly promising and viable clinical biosensor.

3.2.3 Labelled SERS detection

SERS can be employed for label-free detection where molecule that inherently possess high Raman scattering cross section. In most of the cases, detection and interpretation of SERS spectra of biomolecules in a complex biological medium is difficult. Identification of a particular bio-

analyte of interest is not trivial, especially when looking for the detection of trace amount. Labelled SERS sensing for medical and bioanalytical applications is similar to the concept of labelling with dyes or quantum dots in fluorescence studies. Biosensing with the use of SERS labels can be achieved with three major components, such as (i) Raman reporter molecules that has inherently high Raman scattering cross section to provide characteristic Raman peaks as readout; (ii) colloidal noble metal NPs with strong electromagnetic fields to enhance the Raman signal and (iii) a ligand anchored onto the nanoconstruct for recognizing the corresponding target molecule. This section covers the recent advancements in biosensing using SERS-active PCF probes.

Epidermal growth factor receptors

Epidermal growth factor receptors (EGFRs) are proteins that are up-regulated in many cancers and are used as a common clinically significant biomarker. Most commonly used detection methods of EGFR include ELISA and fluorescence sensing. However, ELISA is time-consuming, relatively tedious and has typical detection limit in the µg-ng range, while fluorescence suffers from spectral overlap and photo-bleaching. Further, early detection and diagnosis are crucial for cancer treatment and hence a highly sensitive biosensor is in great demand. In this context, Dinish *et al.* first demonstrated the use of a HC-PCF (HC 800-01, NKT Photonics) to detect EGFR in a cell lysate using anti-EGFR antibody conjugated SERS nanotags as sensing probe with a detection limit ~100 pg/mL and in a sample volume of ~10 nL [25]. SERS nanotag was constructed by anchoring malachite green isothiocyanate (MGITC), a highly Raman-active molecule, as a reporter molecule onto 60nm AuNPs, followed by biconjugation. In this study, eight centimeter long HC-PCF was cleaved at both ends and filled with poly-L-lysine (PLL) followed by cell lysate solutions to anchor the protein inside the hollow core of the fiber. Finally, the antibody conjugated SERS nanotag was infiltrated into the fiber for sensing the immobilized EGFR. The fiber was dried prior to measurement to achieve proper light guidance inside the core at 633 nm. Although this sensor could successfully detect the biomarker from cell lysate with high sensitivity, it lacks practicability as any conventional sensor would demand that the sensing probe (here, SERS nanotags) should be immobilized first and target analyte to be flowed in later.

In a follow up study, same research team demonstrated multiplex detection of hepatocellular carcinoma (HCC) biomarkers using antibody-conjugated MGITC and Cyanine5 (Cy5) SERS

nanotags in a HC-PCF probe (Figure 8) [4]. These nanotags were easily differentiable, as they possess at least two distinct spectral peaks to realize multiplex detection. Using these bioconjugated SERS nanotags, simultaneous multiplex detection of alpha-fetoprotein (AFP) and alpha-1 antitrypsin (A1AT) biomarkers were successfully achieved in a sample volume of ~20 nL at 785 nm. This is of particular significance as the average survival rate of HCC patients is four months after the onset of symptoms. So the successful multiplex detection of A1AT and AFP represents a move towards potential early detection and monitoring. In this study also target protein from cell lysate was immobilized inside the fiber prior to the incorporation of sensing probe in the form of SERS nanotags. An ideal solution would be to design a ready-to-use PCF probe that allows the clinician to incorporate liquid-analyte directly into the bio-functionalized fiber prior to the direct measurement.

Sialic acid

Sialic acids are class of sugars that are found on all cell surfaces that mediate/modulate normal and pathological processes [61]. Their overexpression on cell surfaces can indicate malignant and metastatic phenotypes for various types of cancers. In addition, when overexpressed, sialic-acid rich glycoproteins drives late-stage cancer cells to enter the bloodstream, allowing the cancer to spread further. Tumor malignancy and metastasis could also be easily studied by accurately measuring and monitoring the sialic acid expression within a cell. Commonly used detection methods such as colorimetric/fluorometric analysis, chromatography and potentiometry lack high sensitivity and are also affected by photo-bleaching.

To address this limitation, recently Gong *et al.* developed a SiC-PCF based SERS sensor to detect sialic acid in a single HeLa cell. Initially they compared the SERS performance of HC-PCF and in-house SiC-PCF using a mixture of 60 nm AuNPs and 2-napthalenethiol, which is a common Raman tag [24]. The SiC-PCF exhibited six times stronger signal than that from HC-PCF when excited at 633 nm laser. Subsequently, for the detection of sialic acid, 4-(dihydroxyborophenyl) acetylene (DBA) was anchored onto HeLa cells as Raman readout molecule. HeLa cells generally overexpress sialic acid receptors. As shown in Figure 9, DBA exhibits a strong alkyne Raman peak around 2000 cm^{-1}, which is away from crowded Raman finger print region from HeLa cells and

silica and it can be monitored for the detection of sialic acid. This SiC-PCF sensor could achieve an unprecedented sensitivity by detecting 2.514 fmol of sialic acid on a single cell. This study proves the tremendous potential of SiC-PCF in realizing an ultra-sensitive biosensor.

Lipid peroxidation

Lipid peroxidation is the oxidative degradation of poly-saturated lipids. It is a natural process occurring in small amounts in the body, triggered by reactive oxygen species (ROS). However, if the formation of ROS outpaces the antioxidant capacity of cells, the oxidative stress leads to tissue and organ damage. This is a crucial step in the pathogenesis of diseases such as cancers, neurodegenerative disorders, and atherosclerosis, as well as in aging [62]. Lipid peroxidation modifies proteins in cells by adding an alkyne group. Therefore, the intensity of the Raman alkyne peak can be used to monitor the degree of lipid peroxidation. This alkyne peak is particularly useful for detection as it is isolated from the region associated with cells, which make lipid peroxidation a prime candidate for SERS-based sensing. An in-house seven centimeter long SiC-PCF was filled with a mixture of 60 nm AuNPs and HepG2 liver cancer cells treated with linoleamide alkyne (LAA) and excited at 633 nm to obtain SERS measurement of LAA alone [63]. Then, different concentrations of cumene hydroperoxide (CH) was added to the previous mixture as CH induces lipid peroxidation. These samples were compared with cells treated with only LAA. The alkyne peak intensity increased with CH concentration was able to detect it as low as 5 µM onwards and then showing a steady increase, whereas for the cells treated with LAA alone, the peak was negligible, demonstrating the specificity of the detection method. This SERS-active PCF probe is quite promising for clinical applications as it allows rapid monitoring of lipid peroxidation while avoiding the time consuming preparation of commonly employed staining procedures.

3.3 Gas sensing with PCF probe

Raman/SERS-active PCFs probes could very well be used as an effective gas sensor to overcome most of the challenges encountered by the conventional sensors. Indeed, the most

commonly used highly sensitive gas sensors are often expensive, bulky or unable to provide real-time data. In addition, they tend to lack molecular specificity, which limits the multiplex gas sensing. Raman spectroscopy could be an ideal solution for multiplex gas sensing of complex mixtures, provided it could overcome the inherent sensitivity limitation. In this context, Buric *et al.* proposed a Raman-active HC-PCF probe for sensitive gas/vapor detection for environmental applications [1]. They demonstrated that a 1.5 m long HC-PCF (HC-580-01, NKT Photonics) could enhance Raman signal 130 times more than that in free space when excited by a 514.5 nm laser. They could also successfully detect methane, ethane and propane while mixed in a high-pressure chamber and showed that their PCF-Raman probe could detect these gases effectively at various concentrations.

Later, with the same purpose, Yang *et al.* placed one end of a 30 centimeter long HC-PCF (HC-800B Thorlabs) fiber in a sealed chamber for remote sensing **(**Figure 10 (a)) [3]. A controlled amount of toluene, acetone, and 1,1,1-trichloromethane were placed in the chamber separately in different concentrations for vapor detection. The three analyte were then mixed to test the multiplex gas sensing capabilities of the PCF probe and each gas exhibited clear Raman peaks that allowed their identification (Figure 10 (b)). They achieved an enhancement of ~700 times compared to the conventional detection method using a 785 nm laser.

PCF based sensors are also of great interest for chemical sensing for much the same reasons as they are for biosensing as it can provide fast, accurate detection of trace amounts of compounds within a complex mixtures. It will also offer an additional advantage of the possibility of remote sensing. Furthermore, the interaction length between sample and laser can be much longer than conventional cuvettes or similar cell based setup, thereby improving the sensitivity. In this regard there will be plethora of applications that can be explored in future with SERS/Raman-active PCF sensors.

4. Conclusion and future perspectives

We reviewed recent advancement in the field of PCFs for their use in various biomedical and gas sensing applications using SERS/Raman read out. As far as possible, one should consider of

using SC-PCFs as it has been demonstrated that it provide stronger Raman signal enhancement compared to HC-PCF due to the higher analyte-laser interaction volume. Indeed, Gong *et al.* proved that signal from SiC-PCF was six times stronger than that with HC-PCF [24]. Another advantage of SC-PCF over HC-PCF is that they are not susceptible to a transmission window shift when the holes are filled with liquid-analyte. As mentioned previously, HC-PCFs suffer from spectral shift when both the holes in the cladding and the core are filled with a liquid-analyte. However, in the case of SC-PCF, important Raman peaks of bio-analytes in the 200-800 cm^{-1} range could be masked by the intense Raman peaks of silica. It was quite obvious that the important peaks that could differentiate glucose from fructose was in the 600 -1000 cm^{-1} range [2]. Similarly the differentiation of necrotic, apoptotic and live leukemia cells could only be achieved in the same spectral range [27]. In such cases, the use of HC-PCF is then mandatory. A viable solution to avoid the transmission shift in HC-PCFs could be to use SERS nanotags with capturing moieties to target the specific analyte inside the core and then allow it to dry it prior to measurement, as reported by Dinish *et al.* [4], [25]. However, drying the HC-PCFs may require thermal treatments, which may denature the immobilized bio-analytes such as proteins.

Due to the inherent spectral shift associated with HC-PCF once it is filled with the liquid-analyte and related narrow spectral bandwidth, one should take into consideration that both the excitation and Stokes shifted Raman signals should be within this shifted transmission band. Spectral shift associated with HC-PCF was clearly observed as reported by Tiwari *et al.* [32]. Here, commercial fiber with transmission window centered at 1550 nm was shifted to ~810 nm when it was filled with an aqueous solution of AgNP and Rh6G mixture. This spectral shift allowed exciting the analyte using a commercial 785 nm laser. However, it is impossible to perfectly match the modified transmission bandwidth of commercial HC-PCFs with the laser excitation and Raman wavelength. For example, as reported by Khetani *et al*., for the detection of heparin [56], the transmission window of the commercial HC-PCF was 1430-1610 nm, which was shifted to 717-808 nm when the HC-PCF was filled with the analyte. However, the measured Raman signal was from 975 to 1150 cm^{-1} (i.e. from 850 to 863 nm), which is outside the optimum transmission window resulting in large signal attenuation. This spectral shift prevented in achieving higher sensitivity for the detection of heparin. Better sensitivity could also be realized by a specially designed HC-PCF for guiding the excitation laser and Raman signal once filled with heparin/serum mixture or by using a

Kagome HC-PCF, which possesses a larger transmission window. Another alternative is by using a SC-PCF, where heparin Raman signal is away from the noisy Raman peak of silica.

Even though the implementation of the SERS-active PCF probes are yet to be realized for clinical applications, results from the reported preclinical studies strongly suggest that with further refinement, such probes could potentially be translated to wide variety of diagnostic applications. Some of the potential challenges that need to be carefully addressed to translate a SERS-PCF probe for clinical applications are highlighted here.

The fibers used for SERS sensing are mainly based on enhanced interactions between the light and the analyte. However, they do not take into account of the overall aspects of SERS enhancement. The intensity of collected SERS signal is very much determined by the combined effects of transmission losses (at the wavelengths of the excitation light and scattered Raman signal), the area of light-analyte interactions, the surface for collecting the Raman signal (scattered in all directions) and the coupling efficiency between the fiber, the light source and the Raman spectrometer. The optimizations of the interplays will open up new routes for developing original optical fibers with improved performances for various real life bio-chemical sensing applications. In this prospect, in contrast to the common trend to use SC-PCFs with a very small core, Chen *et al.* have demonstrated the possibility to increase the coverage density of NPs by using a fiber with a very large core could also be explored in detail [64]. Similarly, in fluorescence based fiber-sensing applications, Afshar *et al.* have shown that the highest fluorescence signal is not obtained with the smallest core diameter of the fiber [65]. They have also demonstrated that fiber glass-material with higher refractive index could improve the sensing performances. Even if these results do not take into account of NP interactions, they are nevertheless inspiring for developing optical fiber designs optimized for SERS based sensing applications.

The efficiency and reliability of light couplings into the PCF and into the Raman spectrometer might be significantly improved by tapering down specially designed PCFs. Such PCF-taper will combine optimal core size for efficient SERS interactions in the taper waist and large enough core size for reliable light injection and collection. The relevance of PCF-taper has already been demonstrated in nonlinear optics applications [46], [66]. The future HC-PCFs for SERS sensing

might be based on the anti-resonance or the TIR guiding mechanism for the broader transmission windows with newer fiber designs enabling easier incorporation of the analyte, such as the simplified version of Kagome HC-PCF (composed of only 6 holes [67]) or the recently developed versions composed of one layer of nodeless small tubes [68], [69]. In this prospect, an idealistic fiber would be composed of a hollow-core surrounded by an all-dielectric material cladding, without air holes. Liquid-core Bragg fiber could be suitable, but it suffers from a narrow transmission window [70]. One solution would be to develop a hollow-core fiber with an all-dielectric cladding enabling anti-resonance guidance with a broad transmission window.

Another area that requires tremendous improvement is in overcoming the difficulties associated with the controlled anchoring of metallic NPs inside PCFs. The NPs layer deposited is often not uniform, which leads to inconsistent signal enhancement and hence poor reproducibility. Additionally, methods for robust chemical modification of the inner walls of PCFs for the bio-functionalization, i.e. attaching antibodies or other targeting moieties, is mandatory.

For clinical translation of SERS-PCF probes, a cheap, portable yet sensitive Raman spectrometer/reader with compatible fibers needs to be developed. Eventually, the inherent opto-fluidic properties of PCFs should be translated into a continuous monitoring platform, which could be used in intensive care units, operating theatres or other situations where accurate and real-time monitoring of biological analytes is critical. We can imagine a biopsy needle concept where an all-functionalized and ready-to-use PCF sensor probe is implemented inside the needle. To achieve high specificity for the detection of a targeted biomarker, the NPs anchored inside the PCFs can be specially conjugated with targeting moieties such as antibodies as implemented in labeled SERS approaches. The clinician will only have to collect a very small sample in the range of nanoliter from the patient (sufficient to fill the fiber) and put the needle under the Raman spectrometer for read out, which will eventually minimize the current two-step process of sample collection and readout.

In addition, PCFs can also be integrated with microdevices for sensing applications. Recently, Zhang *et al.* used a SiC-PCF to build an in-line optofluidic Sagnac interferometer in order to detect several analytes using refractive index sensing and as a proof of concept, they detected human

cardiac troponin T [50]. Unterkofler *et al.* analyzed the photoaquation of cyanocobalamin (CNCbl) to aquacobalamin when a solution of CNCbl was exposed to laser excitation inside a HC-PCF in an in-house microfluidic circuitry [71]. In another study Xiao *et al.* used a HC-PCF to fabricate all-in-fiber microcells. They were able to measure the stimulated Raman scattering spectra (SRS) of toluene and ethanol using laser power, which is 6 orders of magnitude lower than that is reported previously, thanks to the high coupling efficiency between the HC-PCF and SMF-28 obtained with their microcells [72]. Khetani *et al.* implemented an HC-PCF in an H-shaped microfluidic differential pressure system when they detected leukemia cells as mentioned above [27]. Though these studies are based on non-Raman/SERS readout, but it illustrates the great potential of PCFs that can be integrated into microfluidic devices/microcells. In this context, SERS-PCF probes could be well adapted in such devices to tap the benefit of flexibility from PCFs and the high sensitivity and multiplex sensing capability of SERS.

Apart from the biochemical sensing domain, SERS-PCF probes could also find tremendous applications in environmental monitoring and homeland security. These include the detection of pollutants, water contaminants and air quality testing. Further, sensing of volatile organic compounds in exhaled breathe could very well serve as biomarkers for the detection of various diseases such as cancer, diabetes mellitus or lactose intolerance [73]. SERS-PCFs probes could also be used for therapeutic purposes for the delivery and activation of photodrugs to specific parts of the body accurately and quickly [74]. The superiority of SERS nanotags for sensitive biomarker detection and their advantages over the fluorescent counterparts in terms of multiplexing capability, low toxicity and clearance efficiency is well reported in *in vivo* studies. Hence, such functionalized nanotags could be exploited in the future as readout probe in SERS-PCF sensor to realize a clinically viable, real time sensing tool. In many ways, the ongoing tremendous development in SERS combined with next generation of PCF designs could eventually lead to a rapid, sensitive diagnostic tool for the patient, as a next step in the implementation of personalized biosensors.

Acknowledgements

Authors sincerely appreciate the funding support from Biomedical Research Council (BMRC), Agency for Science Technology and Research (A*STAR), Singapore and PICS project, “Bio-sensing platforms based on specialty optical fibers as practical clinical diagnostic tools” from

CNRS, France. Authors would also like to express their sincere gratitude to Marissa Chua, a summer attachment student in SBIC, A*STAR for her help.

References

[1] M. P. Buric, K. P. Chen, J. Falk, and S. D. Woodruff, App. Opt. **2008**, *47*, 4255.
[2] X. Yang, A. Y. Zhang, D. A. Wheeler, T. C. Bond, C. Gu, and Y. Li, Anal. Bioanal. Chem. **2002**, *402*, 687.
[3] X. Yang, A. S. P. Chang, B. Chen, C. Gu, and T. C. Bond, Sens. Actuators B-Chem. **2013**, *176*, 64.
[4] U. S. Dinish, G. Balasundaram, Y. T. Chang, and M. Olivo, J. Biophotonics **2014**, *7*, 956.
[5] J. S. W. Mak, A. A. Farah, F. Chen, and A. S. Helmy, ACS Nano **2011**, *5*, 3823.
[6] K. C. Bantz, A. F. Meyer, N. J. Wittenberg, H. Im, O. Kurtulus, S. H. Lee, N. C. Lindquist, S. H. Oh and C. L. Haynes, Phys. Chem. Chem. Phys. **2011**, *13*, 11551.
[7] R. A. Alvarez-Puebla and L. M. Liz-Marzán, Small **2010**, *6*, 604.
[8] S. Laing, K. Gracie, and K. Faulds, Chem. Soc. Rev. **2016**, *45*, 1901.
[9] T. Kang, S. M. Yoo, I. Yoon, S. Y. Lee, and B. Kim, Nano Lett. **2010**, *10*, 1189.
[10] K. K. Maiti, U. S. Dinish, A. Samanta, M. Vendrell, K. S. Soh, S. J. Park, M. Olivo and Y. T. Chang, Nano Today **2012**, *7*, 85.
[11] M. Vendrell, K. K. Maiti, K. Dhaliwal, and Y. T. Chang, Trends Biotechnol. **2013**, *31*, 249.
[12] K. W. Kho, C. Y. Fu, U. S. Dinish, and M. Olivo, J. Biophotonics **2011**, *4*, 667.
[13] W. Xie and S. Schlücker, Phys. Chem. Chem. Phys. **2013**, *15*, 5329.
[14] B. Shan, Y. Pu, Y. Chen, M. Liao, and M. Li, Coord. Chem. Rev. **2018**, *371*, 11.
[15] D. Tsoutsi, M. Sanles-Sobrido, A. Cabot, and P. R. Gil, Curr. Med. Chem. **2018**, *25*, 4638.
[16] M. G. Albrecht and J. A. Creighton, J. Am. Chem. Soc. **1977**, *99*, 5215.
[17] D. L. Jeanmaire and R. P. Van Duyne, J. Electroanal. Chem. **1977**, *84*, 20.
[18] M. Moskovits, J. Raman Spectrosc. **2005**, *36*, 485.
[19] S. Nie and S. R. Emory, Science **1997**, *275*, 1102.
[20] H. Ko, S. Singamaneni, and V. V. Tsukruk, Small **2008**, *4*, 1576.
[21] G. J. Kovacs, R. O. Loutfy, P. S. Vincett, C. Jennings, and R. Aroca, Langmuir **1986**, *2*, 689.
[22] G. Chumanov, K. Sokolov, B. W. Gregory, and T. M. Cotton, J. Phys. Chem. **1995**, *99*, 9466.
[23] J. P. Camden, J. A. Dieringer, J. Zhao, and R. P. Van Duyne, Acc. Chem. Res. **2008**, *41*, 1653.
[24] T. Gong, Y. Cui, D. Goh, K. K. Voon, P. P. Shum, G. Humbert, J. Auguste, Q. X. Dinh, K. Yong, and M. Olivo, Biosens. and Bioelectron. **2015**, *64*, 227.
[25] U. S. Dinish, C. Y. Fu, K. S. Soh, B. Ramaswamy, A. Kumar, and M. Olivo, Biosens. Bioelectron. **2012**, *33*, 293.
[26] A. Khetani, J. Riordon, V. Tiwari, A. Momenpour, M. Godin, and H. Anis, Opt. Express **2013**, *21*, 12340.
[27] A. Khetani, A. Momenpour, E. I. Alarcon, and H. Anis, Biomed. Opt. Express **2015**, *6*, 4599.

[28] F. M. Cox, A. Argyros, M. C. J. Large, and S. Kalluri , Opt. Express **2007**, *15*, 13675.
[29] H. Yan, C. Gu, C. Yang, J. Liu, G. Jin, J. Zhang, L. Hou, and Y. Yao , Appl. Phys. Lett. **2006**, *89*, 204101.
[30] Y. Han, S. Tan, M. K. K. Oo, D. Pristinski, S. Sukhishvili, and H. Du , Adv. Mater. **2010**, *22*, 2647.
[31] D. Yan, J. Popp, M. W. Pletz, and T. Frosch, ACS Photonics **2017**, *4*, 138.
[32] V. S. Tiwari, A. Khetani, M. Naji, and H. Anis, in: *2009 IEEE Sensors*, Christchurch, New Zealand, 2009, p. 367.
[33] P. S. J. Russell, Science **2003**, *299*, 358.
[34] P. S. J. Russell, J. Light. Technol. **2006**, *24*, 4729.
[35] J. C. Knight, Nature **2003**, *424*, 847.
[36] G. Bouwmans, F. Luan, J. C. Knight, and P. S. J. Russell, Opt. Express **2003**, *11*, 1613.
[37] P. J. Roberts, F. Couny, H. Sabert, B. J. Mangan, D. P. Williams, L. Farr, M. W. Mason, and A. Tomlinson, Opt. Express **2005**, *13*, 236.
[38] T. A. Birks, D. M. Bird, T. D. Hedley, J. M. Pottage, and P. S. J. Russell, Opt. Express **2004**, *12*, 69.
[39] G. Antonopoulos, F. Benabid, T. A. Birks, D. M. Bird, J. C. Knight, and P. S. J. Russell, Opt. Express **2006**, *14*, 3000.
[40] G. Humbert, J. C. Knight, G. Bouwmans, P. S. J. Russell, Opt. Express **2004**, *12*, 1477.
[41] F. Couny, F. Benabid, P. J. Roberts, P. S. Light, and M. G. Raymer, Science **2007**, *318*, 1118.
[42] F. Benabid, Science **2002**, *298*, 399.
[43] B. M. Trabold, R. J. R. Hupfer, A. Abdolvand, and P. S. J. Russell, Opt. Lett. **2017**, *42*, 3283.
[44] S. Yiou, P. Delaye, A. Rouvie, J. Chinaud, R. Frey, G. Roosen, P. Viale, S. Février, P. Roy, J. Auguste, and J. Blondy, Opt. Express **2005**, *13*, 4786.
[45] R. Altkorn, I. Koev, R. P. Van Duyne, and M. Litorja, App. Opt. **1997**, *36*, 8992.
[46] S. G. Leon-Saval, T. A. Birks, W. J. Wadsworth, P. S. J. Russell, and M. W. Mason, Opt. Express **2004**, *12*, 2864.
[47] Y. Zhang, D. Yong, X. Yu, L. Xia, D. Liu, and Y. Zhang , Plasmonics **2013**, *8*, 209.
[48] I. Shavrin, S. Novotny, and H. Ludvigsen, Opt. Express **2013**, *21*, 32141.
[49] N. Zhang, G. Humbert, T. Gong, P. P. Shum, K. Li, J. Auguste, Z. Wu, D. J. J. Hu, F. Luan, Q. X. Dinh, M. Olivo, and L. Wei, Sens. Actuators B-Chem. **2016**, *223*, 195.
[50] N. Zhang, K. Li, Y. Cui, Z. Wu, P. P. Shum, J. Auguste, Q. X. Dinh, G. Humbert, and L. Wei, Lab. Chip **2018**, *18*, 655.
[51] J. M. Moison, A. M. Apetrei, J. A. Levenson, G. Mélin, P. Pédeboscq, A. Fleureau, S. Lempereur, and L. Gasca, Opt. Express **2005**, *13*, 1193.
[52] A. M. Apetrei, M. C. P. Huy, N. Belabas, J. A. Levenson, J. M. Moison, J. M. Dudley, G. Mélin, A. Fleureau, L. Galkovsky, and S. Lempereur, Opt. Express **2008**, *16*, 20648.
[53] Y. Guo, M. K. Khaing Oo, K. Reddy, and X. Fan, ACS Nano **2012**, *6*, 381.
[54] Y. Zhang, C. Shi, C. Gu, L. Seballos, and J. Z. Zhang, Appl. Phys. Lett. **2007**, *90*, 193504.
[55] M. K. Khaing Oo, Y. Han, J. Kanka, S. Sukhishvili, and H. Du, Opt. Lett. **2010**, *35*, 466.
[56] A. Khetani, V. S. Tiwari, A. Harb, and H. Anis, Opt. Express **2011**, *19*, 15244.
[57] B. M. Philip, J. G. Brock-Utne, H. J. M. Lemmens, R. A. Jaffe, and P. E. Shuttleworth, J. Extra Corpor. Technol. **2008**, *40*, 193.
[58] A. J. Berger, T.-W. Koo, I. Itzkan, G. Horowitz, and M. S. Feld, Appl. Opt. **1999**, *38*, 2916.
[59] K. E. Shafer-Peltier, C. L. Haynes, M. R. Glucksberg, and R. P. Van Duyne, J. Am. Chem. Soc. **2003**, *125*, 588.

[60] A. Khetani, V. S. Tiwari, A. Momenpour, and H. Anis, in: *11th IEEE International Conference on Nanotechnology*, Portland, OR, USA, **2011**, p. 973.
[61] A. Varki, Trends Mol. Med. **2008**, *14*, 351.
[62] C. Mylonas et D. Kouretas, IN VIVO **1999**, *13*, 295.
[63] T. Gong, N. Zhang, K. V. Kong, D. Goh, C. Ying, J. Auguste, P. P. Shum, L. Wei, G. Humbert, K. Yong, and M. Olivo, J. Biophotonics **2016**, *9*, 32.
[64] H. Chen, F. Tian, J. Chi, J. Kanka, and H. Du, Opt. Lett. **2014**, *39*, 5822.
[65] S. Afshar V., S. C. Warren-Smith, and T. M. Monro, Opt. Express **2007**, *15*, 17891.
[66] G. Humbert, W. J. Wadsworth, S. G. Leon-Saval, J. C. Knight, T. A. Birks, P. S. J. Russell, M. J. Lederer, D. Kopf, K. Wiesauer, E. I. Breuer, and D. Stifter, Opt. Express **2006**, *14*, 1596.
[67] F. Gérôme, R. Jamier, J. Auguste, G. Humbert, and J. Blondy, Opt. Lett. **2010**, *35*, 1157.
[68] F. Poletti, Opt. Express **2014**, *22*, 23807.
[69] S. Gao, Y. Wang, X. Liu, C. Hong, S. Gu, and P. Wang, Opt. Lett. **2017**, *42*, 61.
[70] H. Qu and M. Skorobogatiy, Appl. Phys. Lett. **2011**, *98*, 201114.
[71] S. Unterkofler, R. J. McQuitty, T. G. Euser, N. J. Farrer, P. J. Sadler, and P. S. J. Russell, Opt. Lett. **2012**, *37*, 1952.
[72] L. Xiao, N. V. Wheeler, N. Healy, and A. C. Peacock, Opt. Express **2013**, *21*, 28751.
[73] A. Krilaviciute, J. A. Heiss, M. Leja, J. Kupcinskas, H. Haick, and H. Brenner, Oncotarget **2015**, *6*, 38643.
[74] A. M. Cubillas, S. Unterkofler, T. G. Euser, B. J. M. Etzold, A. C. Jones, P. J. Sadler, P. Wasserscheid, and P. S. J. Russell, Chem. Soc. Rev. **2013**, *42*, 8629.

Table 1 Overview of the PCF based Raman/SERS sensors and detected bio-chemical analytes

Analyte detected	Type of fiber used	Method of detection	Key facts	References
Rh6G	HC-PCF *(Air-6-800 NKT Photonics)* modified in LC-PCF	SERS (40-60 nm AgNPs) Liquid sample	100x stronger than substrate	[54]
	SC-PCF SuC-PCF SuC-PCF	SERS (35 nm AgNPs) Liquid samples	SuC-PCF: best LOD = $1x10^{-10}$ M	[55]
	HC-PCF *(HC-1550 Thorlabs)*	SERS (60 nm AgNPs) Liquid sample	EF = 300 for fiber and NP combined	[32]

	In-house SiC-PCF	SERS (60 nm AuNPs) Liquid sample	LOD = 50 fM Study on the effect of length	[49]
	In-house flow-through multi-holes capillary	SERS (117 µm AuNPs) Liquid sample	LOD < 100 fM EF = 10^8	[53]
Heparin	5 cm HC-PCF *(HC-1550-04 NKT Photonics)*	Raman spectroscopy Liquid sample	EF = 90 LOD = 12 USP/ mL	[56]
Glucose	8 cm HC-PCF *(Air-6-800 NKT Photonics)*	Raman spectroscopy Dipped end	Low laser power 2mW ● 30s integration time ● 50 nL sample volume ● Distinction between glucose and fructose	[2]
Antibiotics	20 cm HC-PCF *(NKT Photonics)*	Raman spectroscopy Liquid sample	Moxifloxacin 1.7 µM in 4 nL sample	[31]
Adenosine	6 cm HC-PCF (*HC-1550-04 NKT Photonics)*	SERS (60-90 nm AgNPs) Liquid sample	EF=2700	[60]
Leukemia cells	HC-PCF *(HC19-1550 NKT Photonics)*	SERS (60 nm AgNPs) Liquid sample	EF = 2700 ● LOD = 300 cells/mL ● Distinction between necrotic, apoptotic, live cells	[27]
EGFR	8 cm HC-PCF *(HC 800-01 NKT Photonics*)	SERS nanotags (AuNP+MGITC+antibodies anti EGFR) Dried sample	Detection of EGFR antibodies: 100 pg/mL in 10 nL	[25]
	7 cm HC-PCF *(HC19-1550 PCF NKT Photonics)*	3 different SERS nanotags (AuNP+ MGTIC or NT or Cy5+ antibodies anti EGFR) Dried sample	Possibility of multiplexed detection	[4]
Alpha-fetoprotein	7cm HC-PCF *(HC19-1550*	SERS nanotags (AuNP+ Cy5 or MGTIC +	Multiplex detection of AFP	[4]

and alpha-1 antitrypsin	*PCF NKT Photonics)*	antibodies anti-AFP or anti-A1AT) Dried sample	and A1AT in 20 nL sample	
Sialic acid	7 cm in-house SiC-PCF	SERS (60 nm AuNPs) Liquid sample	Signal with SiC-PCF 6x stronger than with HC-PCF ● LOD = 2.5 fmol on a single cell	[24]
Lipid peroxidation	7 cm in-house SiC-PCF	SERS (60 nm AuNPs) Liquid sample	LOD = 5 µM	[63]
Gas sensing	1.5 m HC-PCF (*HC-580-01 NKT Photonics)*	Raman spectroscopy Gas sample	130x stronger than conventional method and multiplexed gas sensing	[1]
	30 cm HC-PCF *(HC-800B Thorlabs)*	Raman spectroscopy Gas sample	700x stronger than conventional method and multiplexed gas sensing	[3]

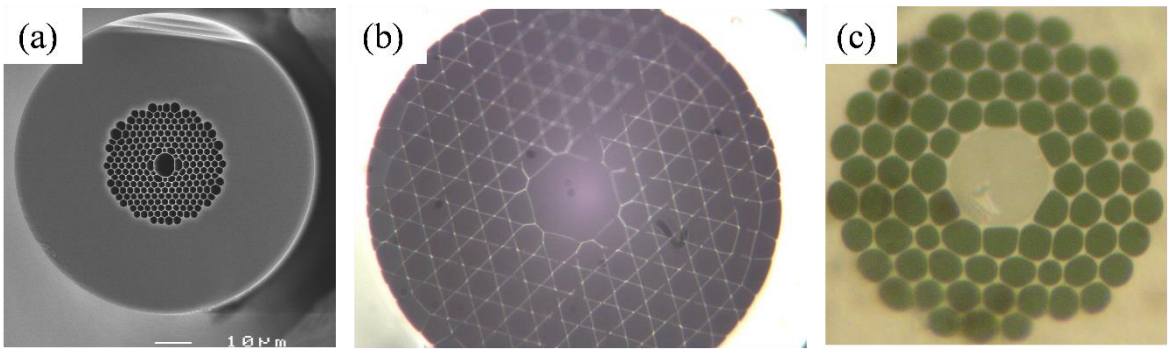

Figure 1 Cross section pictures of **(a)** a HC-PCF with a transmission windows around 850 nm wavelength (Reproduced from [36] with permission of Optical Society of America), **(b)** a Kagome HC-PCF with a broad transmission window around 1000 nm, **(c)** a HC-PCF with the central core filled with ethanol. Air channels are in black. (Reproduced and adapted from [44] with permission of Optical Society of America)

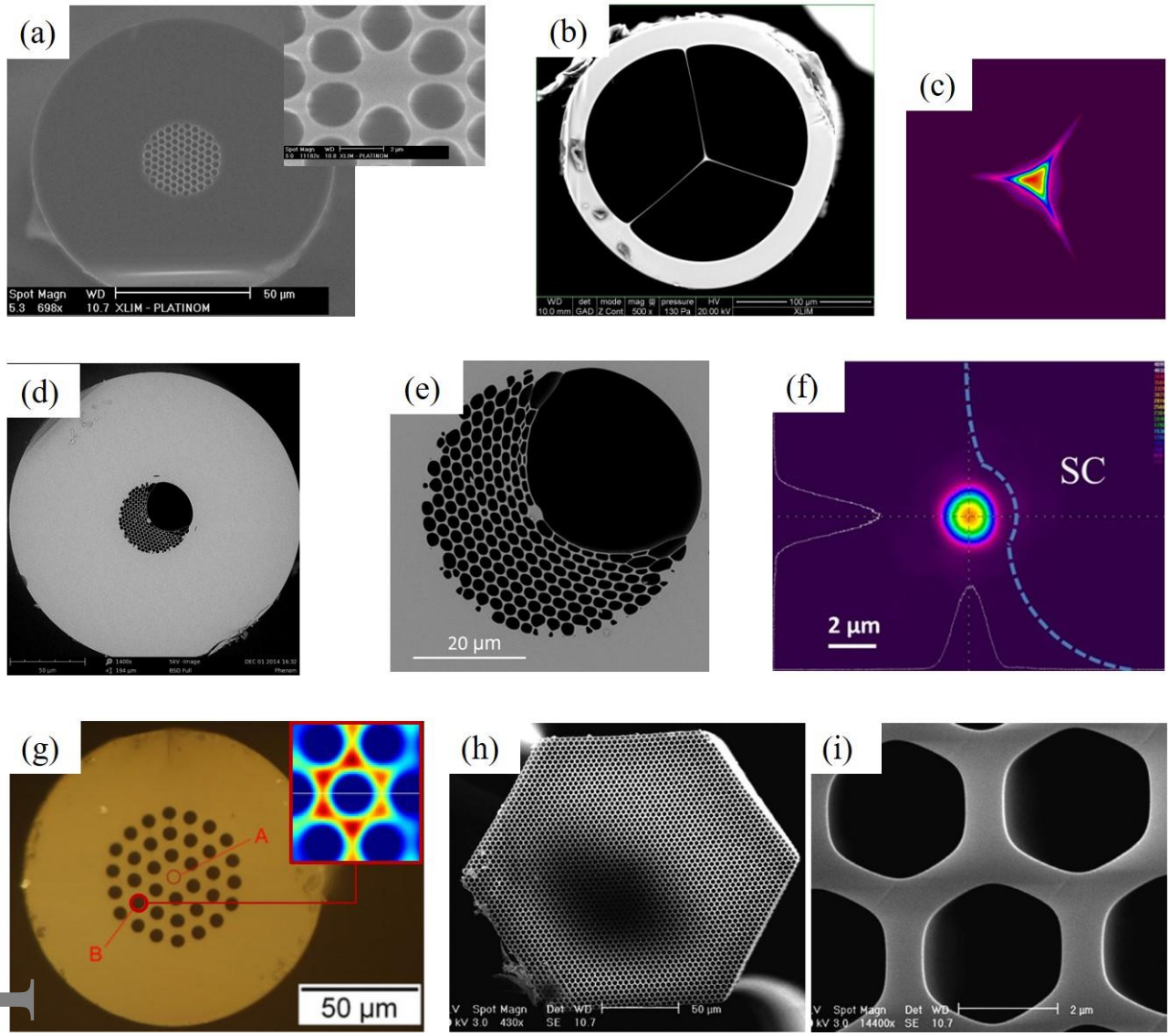

Figure 2 (a) Cross section picture of a SC-PCF composed of a small core diameter (D_{core} < 2 µm), inset: zoom-in the vicinity of the core. **(b)** Cross section picture of a SuC-PCF composed of a small core diameter (< 4 µm) surrounded by three large air-channel ($D_{channel}$ > 70 µm). **(c)** Measured 2D distribution of the light intensity at the output of the SuC-PCF shown in (b). Cross section picture of **(d)** a SiC-PCF and **(e)** zoom-in the micro-structured area composed of a large air-channel ($D_{channel}$ > 20 µm) and a small core diameter (D_{core}< 2.8 µm) (Reproduced and adapted from [49] with permission of Elsevier). **(f)** Measured 2D distribution of the light intensity at the output of the SiC-PCF shown in (d-e) (Reproduced and adapted from [49] with permission of Elsevier). **(g)** Cross section picture of a SC-PCF, inset: 2D distribution of light intensity measured around an air-channel of the photonic crystal cladding (location B) (Reproduced and adapted from [47] with permission of Springer). Cross section picture of **(h)** a PCF composed of only a large photonic crystal (without a central solid core) (Reproduced and adapted from [53] with permission of American Chemical Society), and **(i)** zoom-in few air-channels (Reproduced and adapted from [53] with permission of American Chemical Society).

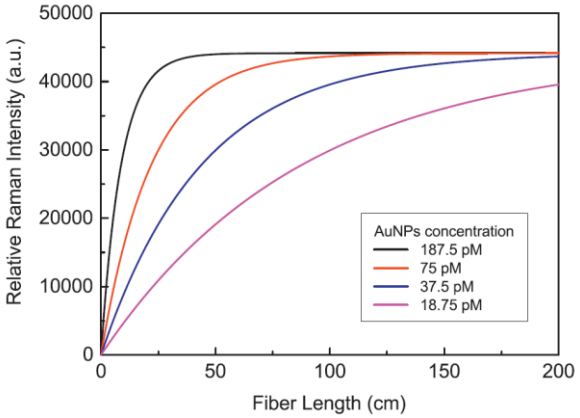

Figure 3 Simulated variations of the relative Raman intensity with fiber length for several concentrations of AuNPs in backward collection setup (Reproduced from [49] with permission of Elsevier)

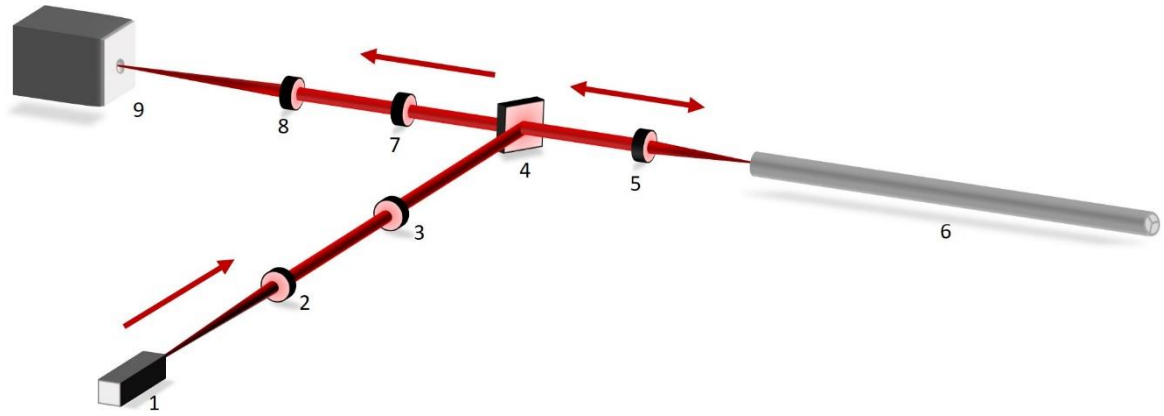

Figure 4 Schematic of the backscattering collection setup often used with PCF probes. 1: Laser; 2: Collimator; 3: Band pass filter; 4: Dichroic Mirror; 5: Microscope objective lens for light coupling; 6: Photonic crystal fiber; 7: Long pass filter; 8: Microscope objective lens for light coupling; 9: spectrometer

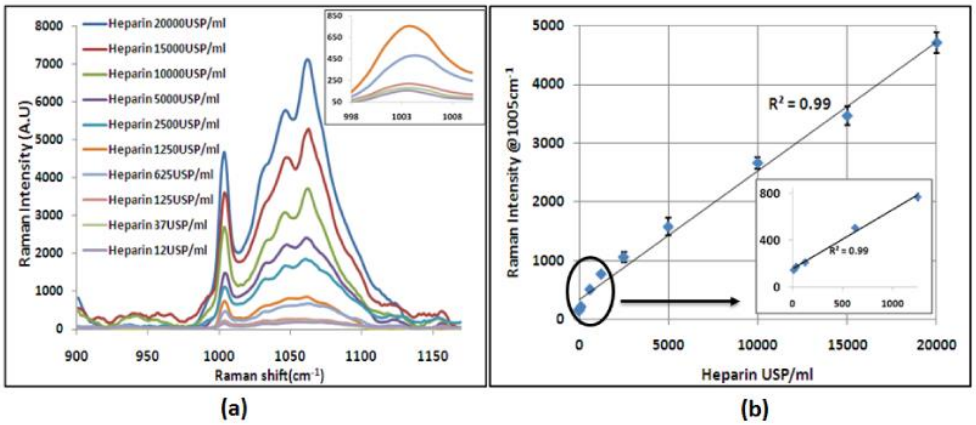

Figure 5 (a) Raman spectra of different concentration of heparin, inset: zoom in on the 1005 cm^{-1} for the lowest concentrations, showing that the peak is still visible. **(b)** Variations of the Raman

intensity of the 1005 cm^{-1} peak with the concentration of heparin, inset: zoom in for the lowest concentrations. (Reproduced from [56] with the permission of Optical Society of America)

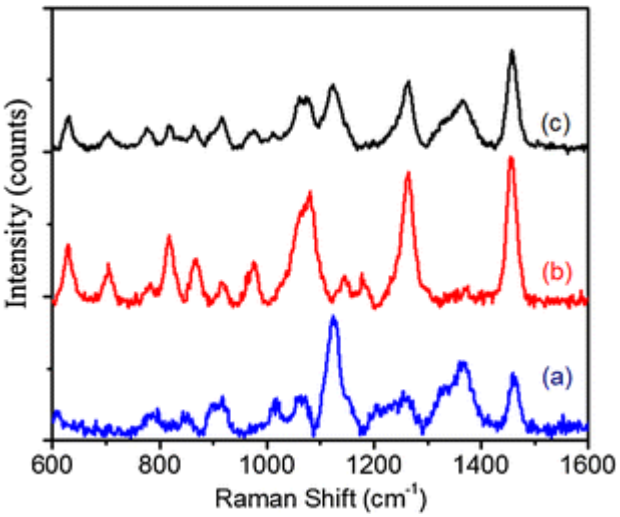

Figure 6 Raman spectra of (a) glucose (10 mM), (b) fructose (10 mM) and (c) a mixture of glucose (5 mM) and fructose (5 mM) measured by the liquid-filled PCF probe allowing the distinction between the two molecules (Reproduced from [2] with permission of Springer Nature)

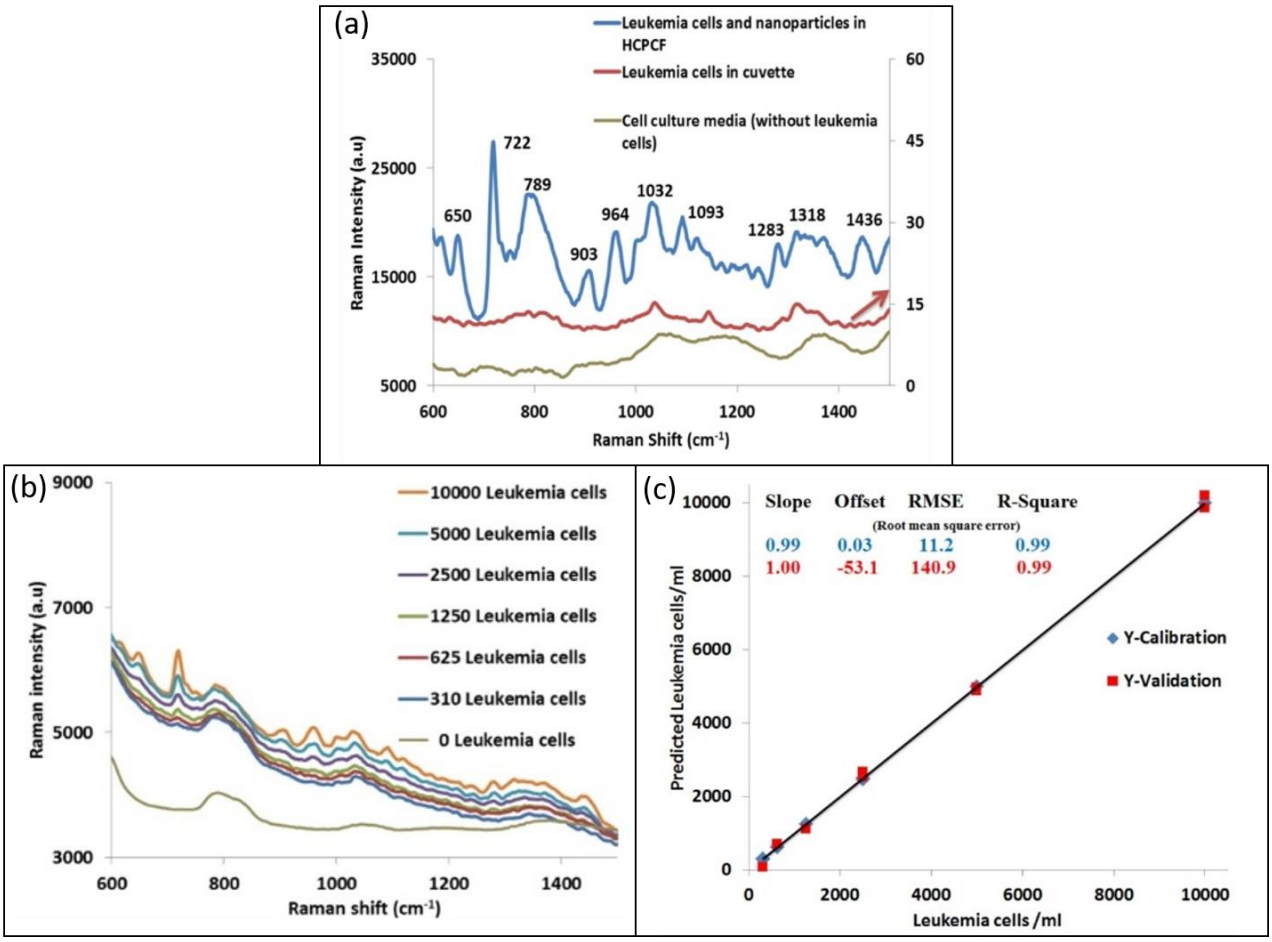

Figure 7 **(a)** Comparison between HL60 cells and AgNPs in HC-PCF and HL60 alone in cuvette: EF = ~2700. **(b)** SERS spectra obtained for different concentrations of live HL60 cells. **(c)** Partial Least Squares prediction of those concentrations showing excellent correlation between calibrated and predicted samples (Adapted and reproduced from [27] with permission of Optical Society of America)

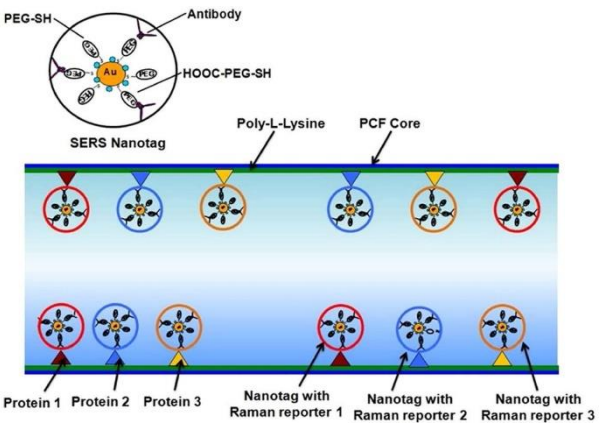

Figure 8 Schematic of multiplex biomarker sensing in a HC-PCF using biofunctionalized SERS nanotags (Reproduced and adapted from [4] with permission of Wiley)

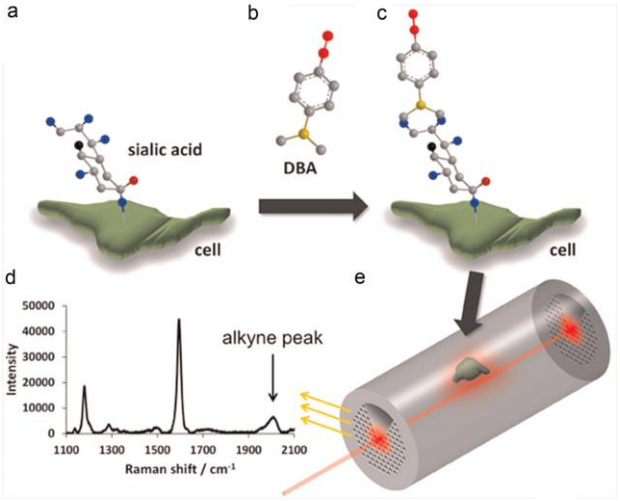

Figure 9 Illustration of the detection of sialic acid using SiC-PCF probe: **(a)** Chemical structure of sialic acid on cell surface. **(b)** Chemical structure of DBA. **(c)** Bonding of DBA and sialic acid on the membrane of a cell. **(d)** Raman spectrum detected from DBA tagged cell in SiC-PCF. **(e)** Schematic of SiC-PCF as a SERS platform for detection of sialic acid on a single cell. (Reproduced from [24] with permission of Elsevier)

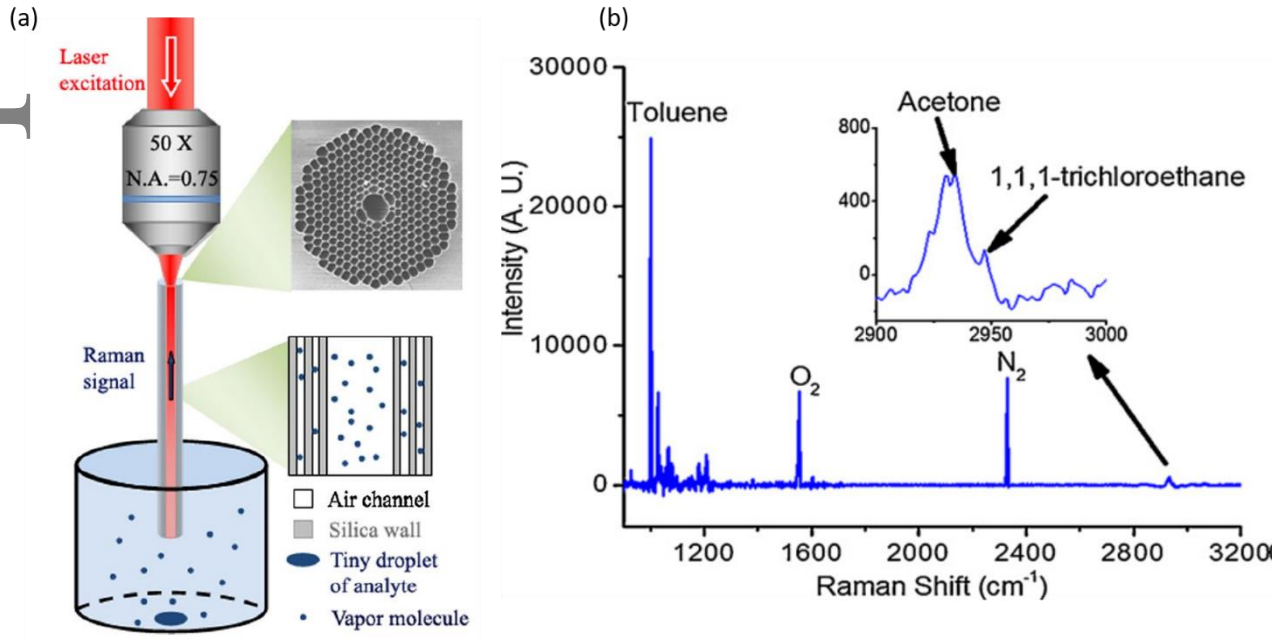

Figure 10 (a) Schematic of the setup used for gas/vapor detection. Top right: SEM picture of a HC-PCF; bottom right: gas molecules inside the core and the cladding air channels of the HC-PCF

(b) Raman spectrum of the mixture of toluene, acetone and 1,1,1-trichloroetane, inset shows the close but differentiable fundamental peaks of acetone and 1,1,1-trichloroetane. (Reproduced and adapted from [3] with permission of Elsevier)